

Multiscale Methods for One Dimensional Wave Propagation with High Frequency Initial Data

Björn Engquist* Henrik Holst† Olof Runborg‡

November 14, 2011

Abstract

High frequency wave propagation problems are computationally costly to solve by traditional techniques because the short wavelength must be well represented over a domain determined by the largest scales of the problem. We have developed and analyzed a new numerical method for high frequency wave propagation in the framework of heterogeneous multiscale methods, closely related to the analytical method of geometrical optics. The numerical method couples simulations on macro- and micro-scales for problems with highly oscillatory initial data. The method has a computational complexity essentially independent of the wavelength. We give one numerical example with a sharp but regular jump in velocity on the microscopic scale for which geometrical optics fails but our HMM gives correct results. We briefly discuss how the method can be extended to higher dimensional problems.

1 Introduction

Any direct simulation of a multiscale problem is computationally very challenging since the smallest scales need to be resolved over domains defined by the largest scale. The heterogeneous multiscale method (HMM) is one computational framework for deriving efficient multiscale methods in which the finest scales are only approximated over small subsets of the full computational domain, [3, 4]. Results from detailed simulations on these microscale domains are used to supply missing data in a numerical macroscale model with an efficient coarse discretization. This missing data typically represents the microscale contribution to macroscale variables.

In [6, 7] and [5] we developed algorithms based on the HMM framework for wave equation problems with highly oscillatory solutions. In these publications the oscillations in the solutions were generated by highly oscillatory coefficients representing the wave velocity. We consider the initial value wave propagation

*Department of Mathematics and Institute for Computational Engineering and Sciences, The University of Texas at Austin, 1 University Station C1200, Austin TX 78712, U.S.A (engquist@ices.utexas.edu).

†Department of Numerical Analysis, CSC, KTH, 100 44 Stockholm, Sweden (holst@kth.se)

‡Department of Numerical Analysis, CSC, KTH, 100 44 Stockholm, Sweden (olofr@nada.kth.se) and Swedish e-Science Research Center (SeRC)

problem,

$$\begin{cases} u_{tt}^\varepsilon - \nabla \cdot (A^\varepsilon \nabla u^\varepsilon) = 0, & \Omega \times [0, T], \\ u^\varepsilon(x, 0) = u_0(x), \quad u_t^\varepsilon(x, 0) = u_1(x) & \forall x \in \Omega. \end{cases}$$

where $\Omega \subset \mathbb{R}^d$ is a bounded, connected domain, and u^ε is Ω -periodic. When the coefficient A^ε is of the form $A^\varepsilon(x) = A(x/\varepsilon)$ and $A(y)$ is periodic the analytic theory of homogenization gives the principles for deriving efficient or homogenized differential equations on the macroscale local averages u of the solution u^ε . The HHM approximations did not require the homogenized equations to be known or the conditions for homogenization theory to be satisfied.

Instead of oscillations in the velocity field, oscillations or high frequencies in initial and boundary values may also generate highly oscillatory solutions. These are very common situations and valid for any high frequency source generation of waves over larger domains in space and time. In these situations local averages are not the appropriate macroscale variables. The local averages do in general not carry essential information and are often zero. Also in this case do the analytical asymptotic theory provide guidance. Geometrical optics, [15], was developed for high frequency wave propagation in smoothly variable velocity fields. The macroscale variables are here the phase ϕ and the amplitude \mathcal{A} ,

$$u = \exp(i\phi(x, t)/\varepsilon)\mathcal{A}(x, t).$$

In our HMM approximation instead of amplitude we use energy E as macroscale variable which allows for a conservative formulation of the macroscale equations,

$$E_t - \nabla \cdot F = 0.$$

In [6, 7] where the oscillations came from heterogeneities in the velocity field we also used a conservative formulation on the macroscale.

We are focusing on the simple one-dimensional scalar wave equation for a proof of concept,

$$\begin{cases} u_{tt}^\varepsilon - \partial_x(a^2 u_x^\varepsilon) = 0, & \Omega \times [0, T], \\ u^\varepsilon(x, 0) = u_0^\varepsilon(x), \quad u_t^\varepsilon(x, 0) = u_1^\varepsilon(x) & \forall x \in \Omega, \end{cases} \quad (1)$$

on an interval $\Omega \subset \mathbb{R}$; Ω -periodic boundary conditions for a and u^ε ; a is smooth and uniformly positive; and $T > 0$ fixed, independent of ε . We assume that a is independent of ε and the initial data u_0^ε and u_1^ε oscillate on a scale proportional to $\varepsilon \ll 1$.

The solution of (1) will be highly oscillating in both time and spatial directions on the scale ε . It is typically computationally costly to solve these kinds of multiscale problems by traditional numerical techniques. The smallest scale must be well represented over a domain, which is determined by the largest scales. These types of variable velocity problems occur for example in simulation of seismic, acoustic and electromagnetic waves.

Geometrical optics (GO) and asymptotic expansions of the solution u^ε to (1) have given rise to many other numerical methods for highly oscillatory problems. Among the more famous ones we have: ray tracing [1, 10] where the system is formulated as a system of ODEs describing the phase and amplitude; wavefront methods [10]. The geometrical optics approach has been generalized in many directions. Since there exists mathematical challenges in the GO model (e.g.,

caustics and focus of rays) other mathematical models have been suggested. For instance a kinetic model [10]; the segment projection method [11]; and Gaussian beams tracing rays containing both amplitude and phase incorporated into one beam [17]. The effect on boundary conditions is included in the geometrical theory of diffraction, [15].

Our contribution is a new heterogeneous multiscale method (HMM) for one-dimensional wave propagation problems with high frequency initial data. The method gives comparable results to geometrical optics [10] when a is smooth. Our aim is to make our method more general than GO. One example is that the method should correctly resolve the effects of jumps in a where a changes values in an $\mathcal{O}(\varepsilon)$ region of the domain Ω . In this case GO does not detect reflections. Our HMM method correctly describes reflection and transmission of energy.

1.1 Geometrical optics

In this section we will give a brief outline of the theory of classical geometrical optics. GO considers single wave solutions to (1) of the form,

$$u^\varepsilon(x, t) = \exp(i\phi(x, t)/\varepsilon)\mathcal{A}(x, t) = \exp(i\phi(x, t)/\varepsilon) \sum_{k=0}^{\infty} A_k(x, t)(i\varepsilon)^k. \quad (2)$$

By inserting (2) into (1) and collecting terms with equal powers of ε , we obtain equations for the unknowns ϕ and A_k . The equation for the phase ϕ is the so called eikonal equation and the equations for the amplitudes A_k are transport equations. The geometrical optics approximation is common in electromagnetic, elastic and acoustic wave propagation [9].

The (formal) series expansion in (2) is called a WKB approximation or the WKB method [15]. It is a general method to find approximations to highly oscillating solutions to partial differential equations where the coefficients vary in space. The WKB method is named after the three physicists Wentzel, Kramers, and Brillouin, who jointly developed it in 1926. The expansion itself does not in general converge, but can still provide us with insight on how to pick good approximations to the solution u^ε .

In the one-dimensional case, we have

$$\begin{cases} u_t^\varepsilon = \exp(i\phi/\varepsilon) \left[\frac{i\phi_t}{\varepsilon} \mathcal{A} + \mathcal{A}_t \right] = \frac{i\phi_t}{\varepsilon} u^\varepsilon + \exp(i\phi/\varepsilon) \mathcal{A}_t, \\ u_x^\varepsilon = \exp(i\phi/\varepsilon) \left[\frac{i\phi_x}{\varepsilon} \mathcal{A} + \mathcal{A}_x \right] = \frac{i\phi_x}{\varepsilon} u^\varepsilon + \exp(i\phi/\varepsilon) \mathcal{A}_x, \end{cases} \quad (3)$$

and

$$\begin{cases} u_{tt}^\varepsilon = \exp(i\phi/\varepsilon) \left[\mathcal{A}_{tt} + \frac{i\phi_{tt}}{\varepsilon} \mathcal{A} + \frac{2i\phi_t}{\varepsilon} \mathcal{A}_t - \frac{\phi_t^2}{\varepsilon^2} \mathcal{A} \right], \\ u_{xx}^\varepsilon = \exp(i\phi/\varepsilon) \left[\mathcal{A}_{xx} + \frac{i\phi_{xx}}{\varepsilon} \mathcal{A} + \frac{2i\phi_x}{\varepsilon} \mathcal{A}_x - \frac{\phi_x^2}{\varepsilon^2} \mathcal{A} \right], \end{cases}$$

which gives us that,

$$\partial_x(a^2 u_x^\varepsilon) = 2aa' u_x^\varepsilon + a^2 u_{xx}^\varepsilon = \exp(i\phi/\varepsilon) \left[\frac{2iaa'\phi_x}{\varepsilon} \mathcal{A} + 2aa' \mathcal{A}_x + a^2 \mathcal{A}_{xx} + \frac{ia^2\phi_{xx}}{\varepsilon} \mathcal{A} + \frac{2ia^2\phi_x}{\varepsilon} \mathcal{A}_x - \frac{a^2\phi_x^2}{\varepsilon^2} \mathcal{A} \right]. \quad (4)$$

By plugging in the expansions of u_{tt}^ε and $\partial_x(a^2 u_x^\varepsilon)$ into (1) and collecting powers of ε we get a set of equations of the form:

$$\begin{aligned} \frac{1}{\varepsilon^2} : & -\phi_t^2 A_0 + a^2 \phi_x^2 A_0 = 0, \\ \frac{i}{\varepsilon} : & \phi_{tt} A_0 + 2\phi_t(A_0)_t - \phi_t^2 A_1 - 2aa' \phi_x A_0 - a^2 \phi_{xx} A_0 \\ & - 2a^2 \phi_x (A_0)_x + a^2 \phi_x^2 A_1 = 0, \\ \varepsilon^k : & (A_k)_{tt} - (a^2 (A_k)_x)_x + 2\phi_t (A_{k+1})_t - 2a^2 \phi_x (A_{k+1})_x \\ & + (\phi_{tt} - (a^2 \phi_x)_x) A_{k+1} + A_{k+2} (-\phi_t^2 + a^2 \phi_x^2) = 0, \quad k \geq 0. \end{aligned}$$

The equation for $\frac{1}{\varepsilon^2}$ gives us the eikonal equation

$$\phi_t^2 - a^2 \phi_x^2 = 0 \quad \Leftrightarrow \quad \phi_t = \pm a \phi_x. \quad (5)$$

We use the fact that $-\phi_t^2 A_1 + a^2 \phi_x^2 A_1 = 0$, to get the equation corresponding to the $\frac{i}{\varepsilon}$ terms,

$$\phi_{tt} A_0 + 2\phi_t (A_0)_t - 2aa' \phi_x A_0 - a^2 \phi_{xx} A_0 - 2a^2 \phi_x (A_0)_x = 0,$$

which can be expressed as,

$$\begin{aligned} (A_0)_t &= \frac{-\phi_{tt} + 2aa' \phi_x + a^2 \phi_{xx}}{2\phi_t} A_0 + \frac{a^2 \phi_x}{\phi_t} (A_0)_x \\ &= \frac{(a^2 \phi_x)_x - \phi_{tt}}{2\phi_t} A_0 \pm a (A_0)_x, \\ &= \pm \frac{a'}{2} A_0 \pm a (A_0)_x, \end{aligned}$$

where we used the fact that,

$$\begin{aligned} \phi_{tt} &= (\pm a \phi_x)_t = \pm a (\phi_t)_x = \pm a (\pm a \phi_x)_x \\ &= aa' \phi_x + a^2 \phi_{xx} = (a^2 \phi_x)_x - aa' \phi_x = (a^2 \phi_x)_x \mp a' \phi_t. \end{aligned}$$

As the final step, to get the equation on conservative form, we multiply both sides with $2A_0$,

$$2A_0 (A_0)_t = \pm a' A_0^2 \pm 2a A_0 (A_0)_x = \pm (a A_0^2)_x.$$

The same computations can be made by matching terms for ε^k ($k \geq 0$),

$$(A_{k+1})_t = \pm \frac{a'}{2} A_{k+1} \pm a (A_{k+1})_x - \frac{(A_k)_{tt} - (a^2 (A_k)_x)_x}{2\phi_t},$$

and by multiplying with $2A_{k+1}$ we get the conservative form,

$$(A_{k+1}^2)_t = \pm (a A_{k+1}^2)_x - \frac{(A_k)_{tt} - (a^2 (A_k)_x)_x}{\phi_t} A_{k+1}.$$

In conclusion, we have,

$$\begin{cases} \phi_t \pm a \phi_x = 0, \\ (A_0^2)_t \pm (a A_0^2)_x = 0, \\ (A_{k+1}^2)_t \pm (a A_{k+1}^2)_x + \frac{(A_k)_{tt} - (a^2 (A_k)_x)_x}{\phi_t} A_{k+1} = 0, \quad k \geq 0. \end{cases} \quad (6)$$

where the \pm sign should be matched, either we have a plus sign or we have a minus on all equations at the same time. The initial data given by $u_0^\varepsilon(x) = A(x, 0)e^{i\phi(x, 0)/\varepsilon}$ leads to the initial conditions:

$$\begin{cases} \phi(x, 0) = \pm \frac{\varepsilon}{i} \log \left(\frac{u^\varepsilon(x, 0)}{|u^\varepsilon(x, 0)|} \right), \\ A_0^2(x, 0) = |u^\varepsilon(x, 0)|^2, \\ A_{k+1}^2(x, 0) = 0, \quad k \geq 0. \end{cases}$$

If the initial data for the phase solves,

$$\phi_x(x, 0) = \pm \frac{1}{a}, \quad (7)$$

in the one-dimensional case the solution to the eikonal equation (5) is very simple, namely $\phi(x, t) = \phi(x, 0) \pm t$. The solution will have a plus sign for the right going phase and a minus sign for the left going phase. We call this kind of ϕ a matched phase for a .

2 Asymptotics for important quantities

In this section we will consider waves going in both left and right directions. We will show asymptotic expansions for the amplitude; scaled energy E ; and the scaled left and right going fluxes F^L and F^R .

Throughout this section we will use the WKB expansion of u^ε for bi-directional wave propagation,

$$u^\varepsilon(x, t) = \mathcal{A}(x, t)e^{i\alpha(x, t)/\varepsilon} + \mathcal{B}(x, t)e^{i\beta(x, t)/\varepsilon}, \quad (8)$$

where

$$\mathcal{A}(x, t) = \sum_{k=0}^{\infty} A_k(x, t)(i\varepsilon)^k, \quad \mathcal{B}(x, t) = \sum_{k=0}^{\infty} B_k(x, t)(i\varepsilon)^k,$$

and α and A_k solves the + version and β and B_k solves the - version of (6). Hence,

$$\begin{cases} \alpha_t + a\alpha_x = 0, \\ \beta_t - a\beta_x = 0. \end{cases} \quad (9)$$

The phases α and β thus correspond to right and left going waves, respectively. We use the notation z^* for the complex conjugate of z .

2.1 Amplitude and energy

In this section we want to describe the leading terms proportional to $1, \varepsilon$ and ε^2 of the square amplitude of the solution u^ε to (1). We will also compute the asymptotic expansion of the energy E of the solution. We define the scaled pointwise energy $E(x, t)$ for the solution u^ε to (1) as,

$$E(x, t) = \frac{\varepsilon^2}{2} |u_t^\varepsilon(x, t)|^2 + \frac{\varepsilon^2 a^2(x)}{2} |u_x^\varepsilon(x, t)|^2. \quad (10)$$

The total energy is preserved in the sense that,

$$\int_{\Omega} E(x, t) \, dx = \int_{\Omega} E(x, 0) \, dx, \quad t \geq 0.$$

By using the WKB expansion (8) we have for the square amplitude of u^ε ,

$$\begin{aligned} |u^\varepsilon|^2 &= |\mathcal{A}|^2 + |\mathcal{B}|^2 + 2\Re \left\{ \mathcal{A}\mathcal{B}^* e^{i(\alpha-\beta)/\varepsilon} \right\} \\ &= |A_0 + i\varepsilon A_1 + \mathcal{O}(\varepsilon^2)|^2 + |B_0 + i\varepsilon B_1 + \mathcal{O}(\varepsilon^2)|^2 + 2\Re \left\{ \mathcal{A}\mathcal{B}^* e^{i(\alpha-\beta)/\varepsilon} \right\}. \end{aligned}$$

We use the fact that,

$$\begin{aligned} \Re \left\{ \mathcal{A}\mathcal{B}^* e^{i(\alpha-\beta)/\varepsilon} \right\} &= \Re \left\{ (A_0 B_0 + i\varepsilon A_1 B_0 - i\varepsilon A_0 B_1 + \mathcal{O}(\varepsilon^2)) e^{i(\alpha-\beta)/\varepsilon} \right\} \\ &= A_0 B_0 \cos \frac{\alpha - \beta}{\varepsilon} + \varepsilon (A_0 B_1 - A_1 B_0) \sin \frac{\alpha - \beta}{\varepsilon} + \mathcal{O}(\varepsilon^2), \end{aligned}$$

which gives us the result we are looking for,

$$\begin{aligned} |u^\varepsilon|^2 &= A_0^2 + B_0^2 + 2A_0 B_0 \cos \frac{\alpha - \beta}{\varepsilon} + \\ &\quad 2\varepsilon (A_0 B_1 - A_1 B_0) \sin \frac{\alpha - \beta}{\varepsilon} + \mathcal{O}(\varepsilon^2). \end{aligned} \tag{11}$$

To compute the asymptotics for the energy E we need to compute the asymptotics of both $|u_t^\varepsilon|^2$ and $|u_x^\varepsilon|^2$. We have for $|u_t^\varepsilon|^2$,

$$\begin{aligned} |u_t^\varepsilon|^2 &= \left| \left(\frac{i\alpha_t}{\varepsilon} \mathcal{A} + \mathcal{A}_t \right) e^{i\frac{\alpha}{\varepsilon}} + \left(\frac{i\beta_t}{\varepsilon} \mathcal{B} + \mathcal{B}_t \right) e^{i\frac{\beta}{\varepsilon}} \right|^2 \\ &= \left| \frac{i\alpha_t}{\varepsilon} \mathcal{A} + \mathcal{A}_t \right|^2 + \left| \frac{i\beta_t}{\varepsilon} \mathcal{B} + \mathcal{B}_t \right|^2 + 2\Re \left\{ \left(\frac{i\alpha_t}{\varepsilon} \mathcal{A} + \mathcal{A}_t \right) \overline{\left(\frac{i\beta_t}{\varepsilon} \mathcal{B} + \mathcal{B}_t \right)} e^{i\frac{\alpha-\beta}{\varepsilon}} \right\} \\ &= \left| \frac{i\alpha_t}{\varepsilon} (A_0 + i\varepsilon A_1 - \varepsilon^2 A_2 + \mathcal{O}(\varepsilon^3)) + (A_0)_t + i\varepsilon (A_1)_t + \mathcal{O}(\varepsilon^2) \right|^2 \\ &\quad + \left| \frac{i\beta_t}{\varepsilon} (B_0 + i\varepsilon B_1 - \varepsilon^2 B_2 + \mathcal{O}(\varepsilon^3)) + (B_0)_t + i\varepsilon (B_1)_t + \mathcal{O}(\varepsilon^2) \right|^2 \\ &\quad + 2\Re \left\{ \left(\frac{i\alpha_t}{\varepsilon} \mathcal{A} + \mathcal{A}_t \right) \overline{\left(\frac{i\beta_t}{\varepsilon} \mathcal{B} + \mathcal{B}_t \right)} e^{i\frac{\alpha-\beta}{\varepsilon}} \right\}. \end{aligned}$$

We now consider only the first term in the above expression,

$$\begin{aligned} &\left| \frac{i\alpha_t}{\varepsilon} (A_0 + i\varepsilon A_1 - \varepsilon^2 A_2 + \mathcal{O}(\varepsilon^3)) + (A_0)_t + i\varepsilon (A_1)_t + \mathcal{O}(\varepsilon^2) \right|^2 \\ &= \left| \frac{i\alpha_t}{\varepsilon} A_0 - \alpha_t A_1 - i\varepsilon \alpha_t A_2 + (A_0)_t + i\varepsilon (A_1)_t + \mathcal{O}(\varepsilon^2) \right|^2 \\ &= \left| i \left(\frac{\alpha_t}{\varepsilon} A_0 + \varepsilon (-\alpha_t A_2 + (A_1)_t) \right) - \alpha_t A_1 + (A_0)_t \right|^2 + \mathcal{O}(\varepsilon^2) \\ &= \left| \frac{\alpha_t}{\varepsilon} A_0 + \varepsilon (-\alpha_t A_2 + (A_1)_t) \right|^2 + |-\alpha_t A_1 + (A_0)_t|^2 + \mathcal{O}(\varepsilon^2) \\ &= \frac{\alpha_t^2}{\varepsilon^2} A_0^2 + 2\alpha_t A_0 (-\alpha_t A_2 + (A_1)_t) + (-\alpha_t A_1 + (A_0)_t)^2 + \mathcal{O}(\varepsilon^2). \end{aligned}$$

The second term is on the same form,

$$\frac{\beta_t^2 B_0^2}{\varepsilon^2} + 2\beta_t B_0(-\beta_t B_2 + (B_1)_t) + (-\beta_t B_1 + (B_0)_t)^2 + \mathcal{O}(\varepsilon^2).$$

The last term is expressed as,

$$2\Re \left\{ \left(\frac{i\alpha_t}{\varepsilon} \mathcal{A} + \mathcal{A}_t \right) \overline{\left(\frac{i\beta_t}{\varepsilon} \mathcal{B} + \mathcal{B}_t \right)} e^{i\frac{\alpha-\beta}{\varepsilon}} \right\} = \\ 2\Re \left\{ \left(\frac{\alpha_t \beta_t}{\varepsilon^2} \mathcal{A} \mathcal{B}^* + \mathcal{A}_t \mathcal{B}_t^* + \frac{i(\alpha_t \mathcal{A} \mathcal{B}_t^* - \beta_t \mathcal{A}_t \mathcal{B}^*)}{\varepsilon} \right) e^{i\frac{\alpha-\beta}{\varepsilon}} \right\}.$$

After a similar calculation for $a^2 |u_x^\varepsilon|^2$ we obtain

$$E = \frac{1}{2} \alpha_t^2 A_0^2 + \frac{1}{2} \beta_t^2 B_0^2 + \frac{1}{2} a^2 \alpha_x^2 A_0^2 + \frac{1}{2} a^2 \beta_x^2 B_0^2 + \mathcal{O}(\varepsilon^2) \\ + \Re \left\{ (\alpha_t \beta_t + a^2 \alpha_x \beta_x) \mathcal{A} \mathcal{B}^* + i\varepsilon ((\alpha_t + a^2 \alpha_x) \mathcal{A} \mathcal{B}_t^* - (\beta_t + a^2 \beta_x) \mathcal{A}_t \mathcal{B}^*) e^{i\frac{\alpha-\beta}{\varepsilon}} \right\}.$$

By using the fact that α_t and β_t solve (9) we have, $\alpha_t \beta_t = -a^2 \alpha_x \beta_x$. Hence,

$$E = a^2 \alpha_x^2 A_0^2 + a^2 \beta_x^2 B_0^2 - \varepsilon \sin\left(\frac{\alpha-\beta}{\varepsilon}\right) (\alpha_t A_0 (B_0)_t - \beta_t (A_0)_t B_0 \\ + a^2 \alpha_x A_0 (B_0)_x - a^2 \beta_x (A_0)_x B_0) + \mathcal{O}(\varepsilon^2). \quad (12)$$

When α and β are matched with a this simplifies to

$$E = A_0^2 + B_0^2 - \varepsilon \sin\left(\frac{\alpha-\beta}{\varepsilon}\right) (\alpha_t A_0 (B_0^*)_t - \beta_t (A_0)_t B_0 \\ + a^2 \alpha_x A_0 (B_0)_x - a^2 \beta_x (A_0)_x B_0) + \mathcal{O}(\varepsilon^2).$$

We see from the expression above that the square amplitude $|u^\varepsilon|^2$ is oscillatory in the terms of size $\mathcal{O}(1)$, $\mathcal{O}(\varepsilon)$ and $\mathcal{O}(\varepsilon^2)$; whereas the energy E is only oscillatory in terms of size $\mathcal{O}(\varepsilon)$ and $\mathcal{O}(\varepsilon^2)$. The $\mathcal{O}(1)$ terms of the WKB expansion of energy is slowly varying. In our numerical method we use the energy as a macroscopic quantity since it will be one order less oscillatory.

2.2 Flux

In this section we will derive an advection equation corresponding to the scaled energy E of the solution to (1). We will also compute asymptotic expansions for the involved quantities. To derive the advection equation we note that,

$$\partial_t |z|^2 = \partial_t (z z^*) = z_t z^* + z z_t^* = 2\Re(z z_t^*).$$

Therefore we can express the time derivate E_t as

$$\frac{1}{\varepsilon^2} E_t = \Re(u_t^\varepsilon (u_{tt}^\varepsilon)^*) + a^2 \Re(u_x^\varepsilon (u_{xt}^\varepsilon)^*) \\ = \Re(u_t^\varepsilon \partial_x (a^2 (u_x^\varepsilon)^*) + a^2 u_x^\varepsilon (u_{xt}^\varepsilon)^*) \\ = \Re((u_t^\varepsilon)^* \partial_x (a^2 u_x^\varepsilon) + a^2 u_x^\varepsilon (u_{xt}^\varepsilon)^*) \\ = \Re(\partial_x ((u_t^\varepsilon)^* a^2 u_x^\varepsilon)), \\ = \partial_x [a^2 \Re((u_t^\varepsilon)^* u_x^\varepsilon)].$$

This shows that the advection equation for the energy is in conservative form,

$$E_t = \partial_x F,$$

where the flux F is,

$$F = a^2 \varepsilon^2 \Re((u_t^\varepsilon)^* u_x^\varepsilon). \quad (13)$$

Furthermore, we define the right- and left going fluxes F^R and F^L by

$$F^R = -\frac{a\varepsilon^2}{4}|u_t^\varepsilon - au_x^\varepsilon|^2, \quad F^L = \frac{a\varepsilon^2}{4}|u_t^\varepsilon + au_x^\varepsilon|^2,$$

where we note that,

$$\begin{aligned} F^L + F^R &= \frac{a\varepsilon^2}{4} (|u_t^\varepsilon + au_x^\varepsilon|^2 - |u_t^\varepsilon - au_x^\varepsilon|^2) \\ &= \frac{a\varepsilon^2}{4} (|u_t^\varepsilon|^2 + 2\Re(au_t^\varepsilon(u_x^\varepsilon)^*) + a^2|u_x^\varepsilon|^2 - |u_t^\varepsilon|^2 + 2\Re(au_t^\varepsilon(u_x^\varepsilon)^*) - a^2|u_x^\varepsilon|^2), \\ &= \varepsilon^2 a^2 \Re((u^\varepsilon)_t^* u_x^\varepsilon), \end{aligned}$$

which is the same flux as we defined in (13), hence $F = F^R + F^L$.

We give a motivation to the notation right- and left-going energy flux in the following way: Suppose a is approximately constant in a $\mathcal{O}(\varepsilon)$ neighborhood of x_0 . We can then use the d'Alembert solution formula and approximate,

$$u^\varepsilon \approx u^L + u^R,$$

where u^R and u^L satisfies $u_t^R + au_x^R = 0$ and $u_t^L - au_x^L = 0$. The fact that,

$$u_t^\varepsilon + au_x^\varepsilon \approx u_t^R + au_t^R + u_t^L + au_x^L = u_t^L + au_x^L = 2au_x^L = 2u_t^L,$$

implies that,

$$F^L = \frac{a\varepsilon^2}{4}|u_t^\varepsilon + au_x^\varepsilon|^2 \approx a\varepsilon^2 \Re(u_t^L (u_t^L)^*) = a^2 \varepsilon^2 \Re((u_t^L)^* u_x^L).$$

Similarly we have,

$$F^R = -\frac{a\varepsilon^2}{4}|u_t^\varepsilon - au_x^\varepsilon|^2 \approx -a\varepsilon^2 \Re((u_t^R)^* u_t^R) = a^2 \varepsilon^2 \Re((u_t^R)^* u_x^R).$$

These are thus of the same form as (13) but with u^ε replaced by u^L and u^R .

Let us now derive, asymptotic expansions for the these fluxes. We have

$$u_t^\varepsilon = \left(\frac{i\alpha_t}{\varepsilon} \mathcal{A} + \mathcal{A}_t \right) e^{i\alpha/\varepsilon} + \left(\frac{i\beta_t}{\varepsilon} \mathcal{B} + \mathcal{B}_t \right) e^{i\beta/\varepsilon}$$

and

$$u_x^\varepsilon = \left(\frac{i\alpha_x}{\varepsilon} \mathcal{A} + \mathcal{A}_x \right) e^{i\alpha/\varepsilon} + \left(\frac{i\beta_x}{\varepsilon} \mathcal{B} + \mathcal{B}_x \right) e^{i\beta/\varepsilon}.$$

This shows that

$$u_t^\varepsilon + au_x^\varepsilon = \left(\frac{i(\alpha_t + a\alpha_x)}{\varepsilon} \mathcal{A} + \mathcal{A}_t + a\mathcal{A}_x \right) e^{i\alpha/\varepsilon} + \left(\frac{i(\beta_t + a\beta_x)}{\varepsilon} \mathcal{B} + \mathcal{B}_t + a\mathcal{B}_x \right) e^{i\beta/\varepsilon}.$$

We now apply (9) and expand in powers of ε ,

$$\begin{aligned}
|u_t^\varepsilon + au_x^\varepsilon|^2 &= \left| (\mathcal{A}_t + a\mathcal{A}_x) e^{i\alpha/\varepsilon} + \left(\frac{2ia\beta_x}{\varepsilon} \mathcal{B} + \mathcal{B}_t + a\mathcal{B}_x \right) e^{i\beta/\varepsilon} \right|^2 \\
&= |\mathcal{A}_t + a\mathcal{A}_x|^2 + \left| \frac{2ia\beta_x}{\varepsilon} \mathcal{B} + \mathcal{B}_t + a\mathcal{B}_x \right|^2 \\
&\quad + 2\Re \left\{ (\mathcal{A}_t + a\mathcal{A}_x) \left(-\frac{2ia\beta_x}{\varepsilon} \mathcal{B}^* + \mathcal{B}_t^* + a\mathcal{B}_x^* \right) e^{i(\alpha-\beta)/\varepsilon} \right\} \\
&= \mathcal{O}(1) + \left| \frac{2ia\beta_x}{\varepsilon} (B_0 + \mathcal{O}(\varepsilon)) + \mathcal{O}(1) \right|^2 \\
&\quad + 2\Re \left\{ -\frac{2ia\beta_x}{\varepsilon} (B_0 + \mathcal{O}(\varepsilon)) ((A_0)_t + a(A_0)_x + \mathcal{O}(\varepsilon)) e^{i(\alpha-\beta)/\varepsilon} \right\} \\
&= \frac{4a^2\beta_x^2 B_0^2}{\varepsilon^2} + \frac{4a\beta_x}{\varepsilon} B_0 ((A_0)_t + a(A_0)_x) \sin\left(\frac{\alpha-\beta}{\varepsilon}\right) + \mathcal{O}(1).
\end{aligned}$$

A similar calculation for $|u_t^\varepsilon - au_x^\varepsilon|^2$:

$$\begin{aligned}
|u_t^\varepsilon - au_x^\varepsilon|^2 &= \left| \left(\frac{-2ia\alpha_x}{\varepsilon} \mathcal{A} + \mathcal{A}_t - a\mathcal{A}_x \right) e^{i\alpha/\varepsilon} + (\mathcal{B}_t - a\mathcal{B}_x) e^{i\beta/\varepsilon} \right|^2 \\
&= \left| \frac{-2ia\alpha_x}{\varepsilon} \mathcal{A} + \mathcal{A}_t - a\mathcal{A}_x \right|^2 + |\mathcal{B}_t - a\mathcal{B}_x|^2 \\
&\quad + 2\Re \left\{ (\mathcal{B}_t - a\mathcal{B}_x) \left(\frac{2ia\alpha_x}{\varepsilon} \mathcal{A}^* + \mathcal{A}_t^* - a\mathcal{A}_x^* \right) e^{i(\beta-\alpha)/\varepsilon} \right\} \\
&= \mathcal{O}(1) + \left| -\frac{2ia\alpha_x}{\varepsilon} (A_0 + \mathcal{O}(\varepsilon)) + \mathcal{O}(1) \right|^2 \\
&\quad + 2\Re \left\{ \frac{2ia\alpha_x}{\varepsilon} (A_0 + \mathcal{O}(\varepsilon)) ((B_0)_t - a(B_0)_x + \mathcal{O}(\varepsilon)) e^{i(\beta-\alpha)/\varepsilon} \right\} \\
&= \frac{4a^2\alpha_x^2 A_0^2}{\varepsilon^2} + \frac{4a\alpha_x}{\varepsilon} A_0 ((B_0)_t - a(B_0)_x) \sin\left(\frac{\alpha-\beta}{\varepsilon}\right) + \mathcal{O}(1).
\end{aligned}$$

In conclusion,

$$\begin{cases} F^R = -a^3\alpha_x^2 A_0^2 - \varepsilon a^2\alpha_x A_0 ((B_0)_t - a(B_0)_x) \sin\left(\frac{\alpha-\beta}{\varepsilon}\right) + \mathcal{O}(\varepsilon^2), \\ F^L = a^3\beta_x^2 B_0^2 + \varepsilon a^2\beta_x B_0 ((A_0)_t + a(A_0)_x) \sin\left(\frac{\alpha-\beta}{\varepsilon}\right) + \mathcal{O}(\varepsilon^2). \end{cases}$$

We showed that $F = F^R + F^L$ so the above computations also gives an asymptotic expansion for the scaled flux F , therefore

$$\begin{aligned}
F &= a^3 (\beta_x^2 B_0^2 - \alpha_x^2 A_0^2) \\
&\quad + \varepsilon a^2 \sin\left(\frac{\alpha-\beta}{\varepsilon}\right) (\beta_x B_0 ((A_0)_t + a(A_0)_x) - \alpha_x A_0 ((B_0)_t - a(B_0)_x)) + \mathcal{O}(\varepsilon^2).
\end{aligned}$$

When α and β are matched with a this simplifies to,

$$\begin{cases} F^R = -aA_0^2 - \varepsilon a^2\alpha_x A_0 ((B_0)_t + a(B_0)_x) \sin\left(\frac{\alpha-\beta}{\varepsilon}\right) + \mathcal{O}(\varepsilon^2), \\ F^L = aB_0^2 + \varepsilon a^2\beta_x B_0 ((A_0)_t + a(A_0)_x) \sin\left(\frac{\alpha-\beta}{\varepsilon}\right) + \mathcal{O}(\varepsilon^2), \end{cases}$$

and

$$F = a(B_0^2 - A_0^2) + \varepsilon a^2 \sin\left(\frac{\alpha - \beta}{\varepsilon}\right) \left(\beta_x B_0((A_0)_t + a(A_0)_x) - \alpha_x A_0((B_0)_t - a(B_0)_x) \right) + \mathcal{O}(\varepsilon^2).$$

The $\mathcal{O}(1)$ term will be slowly varying as we see clearly from the computations. The terms of order $\mathcal{O}(\varepsilon)$ and $\mathcal{O}(\varepsilon^2)$ are oscillatory.

2.3 Local mean and kernels

For the scaled energy E and the scaled flux F , we arrived at asymptotic expansions of the form,

$$X^\varepsilon = X_0 + \varepsilon \sin\left(\frac{\beta - \alpha}{\varepsilon}\right) f(x, t) + \mathcal{O}(\varepsilon^2),$$

where f is a slowly varying function. The second term is thus highly oscillatory. In general these kind of terms are undesirable and problematic from a numerical perspective.

Suppose we want to compute X_0 but only have X^ε . We will be able to do that to $\mathcal{O}(\varepsilon^2)$ accuracy if we could average away the oscillatory part. We suggest that we can reduce the oscillations by instead of taking a point sample of $X^\varepsilon(x, t)$ to approximate $X_0(x, t)$, we compute the average,

$$\bar{X}(x, y) = \frac{1}{4\eta\tau} \int_{x-\eta}^{x+\eta} \int_{t-\tau}^{t+\tau} X^\varepsilon(x + \xi, t + \varphi) d\xi d\varphi,$$

for some choice of η and τ depending on the periodicity of the oscillations. This idea can be improved even further by using a smooth kernel,

$$\bar{X}(x, y) = \frac{1}{\tau\eta} \iint K\left(\frac{t}{\tau}\right) K\left(\frac{x}{\eta}\right) X^\varepsilon(x + \xi, t + \varphi) d\xi d\varphi =: (\mathcal{K}X^\varepsilon)(x, t), \quad (14)$$

denoted here as a *local mean value*, with a kernel K . A kernel $K \in \mathbb{K}^{p,q}$ should satisfy the conditions:

$$\begin{cases} \int_{\mathbb{R}} s^i K(s) ds = \delta_i, & 0 \leq i \leq p, \quad \text{supp } K = [-1, 1], \\ \frac{d^i K(s)}{ds^i} = 0, & 0 \leq i \leq q, \quad \text{for both } s = -1 \text{ and } s = 1. \end{cases}$$

We refer to [6] where we used kernels as above for computing averages of oscillatory quantities. We refer to [12] for a mathematical description of the use of kernels for integrating oscillatory integrands. From [12] we also have the following result:

Theorem 1. *Let $X^\varepsilon(t) = X(t, \frac{t}{\varepsilon})$, where X is 1-periodic in the second variable and $\frac{\partial^r X(t, s)}{\partial t^r}$ is continuous for $r = 0, 1, \dots, p-1$. For any $K \in \mathbb{K}^{p,q}$ there exists constants C_1 and C_2 , independent of ε and η such that,*

$$|(K_\eta * X^\varepsilon)(t) - Y(t)| \leq C_1 \eta^p + C_2 \left(\frac{\varepsilon}{\eta}\right)^q,$$

where $K_\tau(x) = \frac{1}{\tau} K\left(\frac{x}{\tau}\right)$ and $Y(t) = \int_0^1 X(t, s) ds$.

To apply Theorem 1 we need to be able to write the oscillatory term on the form $g(x, t, \frac{x}{\varepsilon}, \frac{t}{\varepsilon})$. We can for instance take $g(x, t, \xi, \varphi) = \sin \xi \frac{\alpha(x, t) - \beta(x, t)}{x} f(x, t)$, and assuming $\alpha \neq \beta$, we see that g is smooth in all variables. If $\alpha = \beta$ the oscillatory term disappears completely. However, the function g is not 1-periodic in ξ . Nevertheless, we observe the same dependence on η, τ as in Theorem 1 in our numerical experiments, thus we expect it is possible to reduce the difference to,

$$|X_0(x, t) - \bar{X}(x, t)| = \mathcal{O}(\varepsilon(\frac{\varepsilon}{\eta})^q) + \mathcal{O}(\varepsilon(\frac{\varepsilon}{\tau})^q) + \mathcal{O}(\varepsilon\eta^p) + \mathcal{O}(\varepsilon\tau^p) + \mathcal{O}(\varepsilon^2),$$

by using a smooth kernel for integrating X^ε .

Note that we can make the difference $|X_0 - X^\varepsilon| = \mathcal{O}(\varepsilon^2)$ by choosing the kernel parameters η, τ, p and q as,

$$\eta, \tau \sim \varepsilon^\gamma, \quad \gamma = \frac{1}{p}, \quad \frac{1}{p} + \frac{1}{q} = 1.$$

The same idea can be applied to the square amplitude but we need to use a slightly larger box $\eta, \tau \sim \varepsilon^\gamma$, where $\gamma = \frac{2}{p}$.

We define the quantities,

$$\begin{cases} \bar{E} = \mathcal{K}E, & \bar{A} = \mathcal{K}|u^\varepsilon|^2, \\ \bar{F}^R = \mathcal{K}F^R, & \bar{F}^L = \mathcal{K}F^L, \end{cases}$$

and with the appropriate choices of K, η and τ we have the asymptotic expansions,

$$\begin{cases} \bar{E} = a^2 \alpha_x^2 A_0^2 + a^2 \beta_x^2 B_0^2 + \mathcal{O}(\varepsilon^2), & \bar{A} = A_0^2 + B_0^2 + \mathcal{O}(\varepsilon^2), \\ \bar{F}^R = -a^3 \alpha_x^2 A_0^2 + \mathcal{O}(\varepsilon^2), & \bar{F}^L = a^3 \beta_x^2 B_0^2 + \mathcal{O}(\varepsilon^2). \end{cases}$$

3 The numerical algorithm

In this section we will describe our HMM method for the wave equation (1). We will assume that the initial data is of the form,

$$u_0^\varepsilon(x) = A(x)e^{i\phi(x,0)/\varepsilon}, \quad \text{either } u_1^\varepsilon(x) = 0 \text{ or } u_1^\varepsilon(x) = -\frac{i}{\varepsilon}u_0^\varepsilon(x),$$

where ϕ is matched with a , c.f. (7). The scaled energy E at $t = 0$ is asymptotically equal to $A^2(x) + \mathcal{O}(\varepsilon^2)$.

We will first assume that the phase is matched with a as described in the end of Section 1.1. In Section 3.3 we will discuss how this assumption can be avoided.

We defined the scaled energy E for solutions of (1) as the sum of its kinetic energy and potential energy in (10) and the local mean energy as $\bar{E} = \mathcal{K}E$ in Section 2.3. It is easy to show that ∂_x and ∂_t commutes with the local mean operator \mathcal{K} defined in (14). By applying the mean value operator \mathcal{K} to (13) we obtain the following left hand side,

$$\mathcal{K}(E_t) = \partial_t \mathcal{K}E = \bar{E}_t,$$

and for the right hand side,

$$\mathcal{K}\partial_x F = \partial_x \mathcal{K}F = \partial_x \bar{F}.$$

Thus, we have

$$\bar{E}_t = \partial_x \bar{F}.$$

Inspired by this we choose our macroscopic variables as the local mean right and left going energy \bar{E}^R and \bar{E}^L . They should satisfy that $\bar{E} = \bar{E}^R + \bar{E}^L$ and we assume they solve the PDE:

$$\begin{cases} \bar{E}_t^R - \bar{F}_x^R = 0, & \Omega \times [0, T], \\ \bar{E}_t^L - \bar{F}_x^L = 0, & \Omega \times [0, T], \end{cases} \quad (15)$$

with Ω -periodic boundary conditions in x and initial data

$$\bar{E}^R(x, 0) = \bar{E}^L(x, 0) = \frac{1}{2}(\mathcal{K}E)(x, 0) = \frac{1}{2}A_0^2(x, 0) + \mathcal{O}(\varepsilon^2), \quad \forall x \in \Omega,$$

for bi-directional initial data ($u_t^\varepsilon = 0$), or

$$\begin{cases} \bar{E}^L(x, 0) = 0, & \bar{E}^R(x, 0) = (\mathcal{K}E)(x, 0), & \text{alternatively,} \\ \bar{E}^R(x, 0) = 0, & \bar{E}^L(x, 0) = (\mathcal{K}E)(x, 0), \end{cases}$$

for one-way initial data ($u_t^\varepsilon(x, 0) = -\frac{i}{\varepsilon}u^\varepsilon(x, 0)$). The fluxes \bar{F}^R and \bar{F}^L will be computed from a micro problem based on the expression in Section 2.2.

We need to be careful when discretizing (15) in order to capture transmission and reflection of energy around jumps in the material. We must consider the discretized energy E^R and E^L as the *ingoing* energy to the grid point, e.g., E^R is the ingoing from left energy and travels from left to right. Similarly, E^L is the energy that travels from right to left. For the fluxes we argue as follows: The flux F_R^R is the transmitted flux from the left going energy plus the reflected flux from the left going energy. Moreover, F_L^R is the reflected flux from the right going energy plus the transmitted flux from the right going energy. The quantities F_R^L and F_L^L are defined analogously. We illustrate this in Fig. 1 where we show a numerical example for a jump. The fluxes are sampled for a inbound right ingoing energy $E^R = 1$, with zero ingoing left energy. Note that when a is smooth there will be almost no reflection and only transmitted flux.

Based on this observation we choose to discretize (15) with an upwind scheme for the right and left going energy \bar{E}^R and \bar{E}^L ,

$$\begin{cases} (\bar{E}^R)_m^{n+1} = (\bar{E}^R)_m^n - \lambda((\bar{F}_L^R)_m^n - (\bar{F}_R^R)_{m-1}^n), \\ (\bar{E}^L)_m^{n+1} = (\bar{E}^L)_m^n - \lambda((\bar{F}_L^L)_{m+1}^n - (\bar{F}_R^L)_m^n), \end{cases} \quad \lambda = \frac{\Delta t}{\Delta x}. \quad (16)$$

Next we will describe how to compute all the flux quantities in (16) ($(\bar{F}_R^R)_m^n$, $(\bar{F}_R^L)_m^n$, $(\bar{F}_L^R)_m^n$, $(\bar{F}_L^L)_m^n$, ...) by solving a micro problem with the macroscopic variables $(\bar{E}^R)_m^n$, $(\bar{E}^L)_m^n$, t_n and x_m as input.

3.1 Micro problem

In this section we describe the micro problem which shall provide the macro scheme with the missing information, the flux. The micro problem will be of

the form (1) but without boundary conditions. The input to the micro problem are the macroscopic variables $x_m, t_n, (\bar{E}^R)_m^n$ and $(\bar{E}^L)_m^n$. We will use the notation $\mathcal{E}^R := (\bar{E}^R)_m^n, \mathcal{E}^L := (\bar{E}^L)_m^n$, for the ingoing energy from right and left respectively; $t' := t_n$; and $x' := x_m$ to make the notation simpler.

We make a change of variables in the micro problem such that $x' \mapsto 0$ and $t' \mapsto 0$. This implies that $a(x) \mapsto a(x + x')$. The micro problem is formulated as an initial value problem:

$$\begin{cases} v_{tt}^\varepsilon - \partial_x(a^2 v_x^\varepsilon) = 0, \\ v^\varepsilon(x, 0) = \sqrt{\mathcal{E}^R} \exp(i\alpha(x, 0)/\varepsilon) + \sqrt{\mathcal{E}^L} \exp(i\beta(x, 0)/\varepsilon), \\ v_t^\varepsilon(x, 0) = -\frac{i}{\varepsilon} v^\varepsilon(x, 0), \end{cases} \quad (17)$$

where α, β are matched with a at $t = 0$,

$$\alpha(x, 0) = -\beta(x, 0) = \int_0^x \frac{ds}{a(s)}. \quad (18)$$

We shall now give a motivation to why we choose these initial conditions. In the language of HMM this step $\mathcal{E}^R, \mathcal{E}^L \mapsto v^\varepsilon$ is called the reconstruction step. The approximation should be such that u^ε satisfy the wave equation and u^ε has an energy approximately the same as $\mathcal{E}^R + \mathcal{E}^L$.

The asymptotic solution v^ε to (17) can be written as a bi-directional wave,

$$v^\varepsilon(x, t) \simeq A_0(x, t) \exp(i\alpha(x, t)/\varepsilon) + B_0(x, t) \exp(i\beta(x, t)/\varepsilon). \quad (19)$$

For a one way wave, going right $B_0 = 0$ the local mean (scaled) energy of that solution will then be equal to $A_0^2 + \mathcal{O}(\varepsilon^2)$. Similarly, for a left going one wave, the local mean (scaled) energy will be equal to $B_0^2 + \mathcal{O}(\varepsilon^2)$. We therefore pick $A_0 = \sqrt{\mathcal{E}^R}$ and $B_0 = \sqrt{\mathcal{E}^L}$. The initial condition v_t^ε is chosen to match (19). Indeed,

$$v_t^\varepsilon \approx \frac{i}{\varepsilon} A_0 (\alpha_t \exp(i\alpha/\varepsilon) + \beta_t B_0 \exp(i\beta/\varepsilon)),$$

and by (9) and (19) we have that,

$$v_t^\varepsilon(x, 0) = -\frac{i}{\varepsilon} v^\varepsilon(x, 0).$$

We use a Leapfrog finite difference scheme for (17). It is based on central differences in both time and space. We use a uniform grid such that $\lambda = \frac{\Delta t}{\Delta x}$ is constant. The scheme reads:

$$\begin{cases} v_m^{n+1} = 2v_m^n - v_m^{n-1} + \frac{\Delta t^2}{\Delta x} \left((av_x^\varepsilon)_{m+\frac{1}{2}}^n - (av_x^\varepsilon)_{m-\frac{1}{2}}^n \right), & 0 \leq n < N, \\ \text{where } (av_x^\varepsilon)_{m\pm\frac{1}{2}}^n = \pm \frac{a_{m\pm\frac{1}{2}}}{\Delta x} (v_{m\pm 1}^n - v_m^n). \end{cases} \quad (20)$$

Since we are using a two-step method we require a one-step method to initialize the method. We have chosen to set

$$v_m^{-1} = \underbrace{v^\varepsilon(x_m, 0)}_{=v_0^\varepsilon(x)} - \Delta t \underbrace{v_t^\varepsilon(x_m, 0)}_{=v_1^\varepsilon} + \frac{\Delta t^2}{2} \underbrace{v_{tt}^\varepsilon(x_m, 0)}_{=\partial_x(a^2 v_x^\varepsilon)} + \mathcal{O}(\Delta t^3), \quad (21)$$

where $\partial_x(a^2 v_x^\varepsilon)$ is discretized as above. See [14] for implementation details.

The numerical computation requires a bounded domain Y^ε . We choose a bounded Y^ε such that the effects from the boundary do not reach inside $[-\eta, \eta] \subset Y^\varepsilon$ for $-\tau \leq t \leq \tau$. Typically, to obtain this we use $Y^\varepsilon = [-y_{\max}, y_{\max}]$ with $y_{\max} = \eta + \tau \max a$. Other techniques for numerically simulating infinite domains are standard absorbing boundary conditions (ABC) [8] and perfectly matched layers (PML) [2].

Remark 2. Suppose we have a matched phase ϕ such that $\phi_x = 1/a$ and

$$\phi(x, 0) = \phi(x', 0) + (x - x')\phi_x(x', 0) + \mathcal{O}((x - x')^2).$$

Then it is possible with little loss of asymptotic accuracy to use an approximation of the initial data in (17) of the form,

$$v^\varepsilon(x, 0) \approx \sqrt{\mathcal{E}^R} \exp\left(\frac{i(x - x')}{\varepsilon a(x)}\right) + \sqrt{\mathcal{E}^L} \exp\left(\frac{-i(x - x')}{\varepsilon a(x)}\right). \quad (22)$$

The error in the initial data with respect to the scaled energy \mathcal{E}^R and \mathcal{E}^L will be proportional to ε instead of ε^2 .

3.2 Compression step

Once we have solved (17) for v^ε we obtain the macroscopic unknowns \bar{F}^R and \bar{F}^L by computing the local mean in the point (x', t') , which is just $x = 0$ and $t = 0$ in the local coordinate system,

$$\bar{F}^R \approx -\frac{\varepsilon^2}{4} \mathcal{K} (a|v_t^\varepsilon - av_x^\varepsilon|^2), \quad \bar{F}^L \approx \frac{\varepsilon^2}{4} \mathcal{K} (a|v_t^\varepsilon + av_x^\varepsilon|^2). \quad (23)$$

The quantities u_t^ε and u_x^ε are thus needed at to compute the fluxes. These are computed from the discrete solution u_m^n at time t_n at x_m with a second order finite difference scheme:

$$\begin{cases} (v_t^\varepsilon)_m^{n+1} = \frac{v_m^{n+1} - v_m^{n-1}}{2\Delta t} + \Delta t \partial_x(a^2(x_m)v_x^\varepsilon(x_m, t_n)), & 0 \leq n < N, \\ v_x^\varepsilon(x_m, t_n) = \frac{v_{m+1}^n - v_{m-1}^n}{2\Delta x}, & 0 \leq n \leq N, \end{cases}$$

where $\partial_x(a^2(x_m)v_x^\varepsilon(x_m, t_n))$ is discretized in the same way as in the micro solver.

In the case when we have a jump or sharp variations in a we sample two values for both \bar{F}^R and \bar{F}^L . One value on each side of the jump for each flux. This will represent the ingoing and reflected energy corresponding to which side the inbound energy comes from. To illustrate the idea we show in Fig. 1 a micro problem computation from the numerical example 4.2, where we have a jump in a at $x = 0.5$.

Remark 3. We note that we can precompute the micro problems by observing that, for $\vec{E} = [\bar{E}^R \quad \bar{E}^L]^T$,

$$\begin{cases} \bar{F}^R(x_m, \vec{E}) = \bar{E}^R \bar{F}^R(x_m, e_1) + \bar{E}^L \bar{F}^R(x_m, e_2), \\ \bar{F}^L(x_m, \vec{E}) = \bar{E}^R \bar{F}^L(x_m, e_1) + \bar{E}^L \bar{F}^L(x_m, e_2), \end{cases}$$

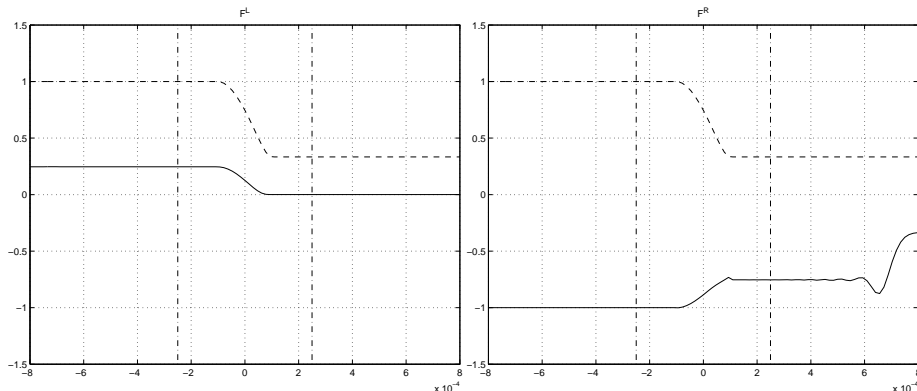


Figure 1: The fluxes F^L (left figure) and F^R (right figure) visualized for an incoming wave from the right, $E^R = 1$, $E^L = 0$. The material a (dashed line) shows the jump in the middle of the microbox (c.f. Section 4.2). The two vertical dashed lines are the sampling points where we compute the right F_R^R and left flux F_L^R . We see in the left figure the reflection at the left side of the jump and in the right picture we see the transmission to the right of the jump.

where

$$e_1^T = [1 \ 0], \quad e_2^T = [0 \ 1].$$

Thus it is enough to compute the matrices S_m for each grid point x_m ,

$$S_m = \begin{bmatrix} \bar{F}^R(x_m, e_1) & \bar{F}^R(x_m, e_2) \\ \bar{F}^L(x_m, e_1) & \bar{F}^L(x_m, e_2) \end{bmatrix}, \quad 0 \leq m \leq M,$$

i.e. solve one micro problem per macro grid point. We then formulate the flux $\bar{F}(x_m, \vec{E})$ for some grid point x_m as a linear mapping via the transfer matrix S_m ,

$$\bar{F}(x_m, \vec{E}) = \begin{bmatrix} \bar{F}^R(x_m, \vec{E}) \\ \bar{F}^L(x_m, \vec{E}) \end{bmatrix} = S_m \vec{E}$$

Note that for smooth $a(x)$ with $|a_x(x)|$ small, S will be almost diagonal. In the case when $a(x)$ has a jump we sample the flux in two places, to the left and to the right of the jump, thus obtaining two different matrices for that grid point, $(S^R)_m$ and $(S^L)_m$, one matrix for each side of the the jump. In the case when we cannot say for sure where there is a jump we can choose to always compute both matrices for each grid point.

3.3 Non matched phase and extensions to higher dimensions

If the phase is not matched to the material one would also need to keep the phase ϕ as a macroscopic variable for each of the waves. Moreover, there should be a way to update it in the HMM procedure. Since the phase is in general not a conserved quantity, it will not satisfy an equation on flux form as the energy. The simplest approach would be to instead just make an ansatz for the macroscopic phase equation as

$$\phi_t = F(x, \phi, \phi_x), \quad (24)$$

where F is some unknown function. It will be important to use a discretization for (24) that has a form that is stable if applied to the effective eikonal equation. Initial data for the micro problem would be given with the current correct phase and energy. To approximate F from the result of the HMM micro problem one would need a method to untangle the phase $\tilde{\phi}$ of the micro problem solution after the short time τ . Then we could take

$$F \approx \frac{\tilde{\phi}(\tau, x) - \phi(0, x)}{\tau}.$$

If $v_\varepsilon \approx A(x, t) \exp(i\phi(x, t)/\varepsilon)$ the untangling would be simply

$$\tilde{\phi}(x, t) \approx \frac{\varepsilon}{i} \log \left(\frac{v_\varepsilon}{|v_\varepsilon|} \right).$$

When v_ε is a sum of several waves, more complicated methods would be required.

The main new difficulty in higher dimensions is the fact that the solution is in general made up of any number of waves going in any directions, not just two waves going backwards and forwards as in one dimension.

One way to treat this case is to explicitly keep track of the directions of the waves and track them individually. Each wave would have its own amplitude and phase. These would be the macroscopic variables. The direction would correspond to the gradient of the phase. To update the amplitudes and phases from the solution of a micro problem one would need a similar untangling step as for the non-matched phase above, but for the more challenging multi-dimensional setting. The problem of untangling phases and amplitudes from a given solution in two and three dimensions has been studied in [?], where methods for this based on local spectral decompositions were presented. This step can also benefit from Gaussian beam technology where a general wave field is decomposed into a number of waves with individual phases and amplitudes [16]. The issue of how to add new waves, which appear for instance at caustics, must also be addressed.

Another way to approach the two-dimensional case would be to consider the energy as a function of angle $E = E(x, t, \theta)$, representing the wave energy propagating in the θ -direction, in analogue with the E^L and E^R energies for the one-dimensional case. In the high frequency limit this energy function satisfies the Liouville equation

$$E_t + v(x, \theta) \cdot \nabla_x E + d(x, \theta) E_\theta = 0,$$

where

$$v(x, \theta) = a(x)(\cos \theta, \sin \theta), \quad d(x, \theta) = \nabla a(x) \cdot (\sin \theta, -\cos \theta).$$

The macroscopic equation would hence be set in one dimension higher than the wave equation, but it would be independent of ε . In an HMM method E would be discretized also in θ . The micro problems would still solve the wave equation. If the phase is not matched to $a(x)$ the quantities $v(x, \theta)$ and $d(x, \theta)$ or their effect on the solution E must also be calculated in the micro step.

4 Numerical experiments

In this section we will demonstrate two numerical experiments. The first experiment falls within the regime where we can compare with geometrical optics

and shows that our method works and is comparable to the GO solution. The second experiment falls outside the regime of GO. We will try to compute the solution to a wave propagation problem where we have a jump in the material whose width is proportional to $\mathcal{O}(\varepsilon)$.

We will always consider initial data of the form

$$u^\varepsilon = A_0 \exp(i\phi/\varepsilon)$$

where ϕ is matched with a and ε is such that

$$\exp(i\phi(0,0)/\varepsilon) = \exp(i\phi(1,0)/\varepsilon) = 1,$$

to make the problem periodic on the macro scale. The initial data for u_t^ε will determine if the wave is one-way or has energy propagating in both the left and right directions.

4.1 Numerical experiment one

In this section we will solve (1) on $\Omega = [0, 1]$ up to T with the material,

$$a(x) = \sqrt{2 + \sin 2\pi x},$$

shown in Fig. 2, and the initial data,

$$u_0^\varepsilon(x) = \sqrt{2}e^{-200(x-0.5)^2} e^{i\phi/\varepsilon}, \quad u_1^\varepsilon(x) = 0,$$

with $\varepsilon = 1.00584466038278 \cdot 10^{-3}$. For finite time T , in the limit $\varepsilon \rightarrow 0$, this problem will also be time periodic with period T ,

$$T = \left(\int_0^1 \frac{dx}{a(x)} \right)^{-1} = 0.71908482829371612 \dots$$

The exact solution u^ε will then at $t = T$ be pointwise equal to the initial data, within some $\mathcal{O}(\varepsilon)$ bound. The choice of ε is such that ϕ will be both matched with a and ε .

Initial data for \bar{E}^L and \bar{E}^R is given as in (15). That is,

$$\bar{E}^R = \bar{E}^L = \frac{1}{4}A_0^2(x) = \frac{1}{2}(e^{-200(x-0.5)^2})^2.$$

We show the initial energy profile in Fig. 3 and the wave itself in Fig 4.

We discretize the GO equations (6) with a first order accurate upwind scheme,

$$\begin{cases} \phi_m^{n+1} = \phi_m^n - \lambda a(x_m) (\phi_m^n - \phi_{m-1}^n) \\ (A^2)_m^{n+1} = (A^2)_m^n - \lambda (F_m^n - F_{m-1}^n), \\ F_m^n = a(x_m)(A^2)_m^n, \end{cases} \quad (25)$$

where $\lambda = \frac{\Delta t}{\Delta x}$ is constant and the initial data is given in (6). The HMM energy is discretized with the scheme (16).

We discretize u^ε such that $u^\varepsilon(m\Delta x, n\Delta t) \approx u_m^n$. The discrete function u_m^n is given by the same scheme described in Section 3.1. We use the following numerical parameters: $\rho := \frac{\varepsilon}{\Delta x} = 32$, $\lambda := \frac{\Delta t}{\Delta x} = 0.5$, such that the CFL number is $\frac{\sqrt{3}}{2} \approx 0.86603$. In Fig. 5 we show a result of a computation up to $t = T$. We can see that the coarse scale solutions (GO, HMM) are close compared to the DNS solution.

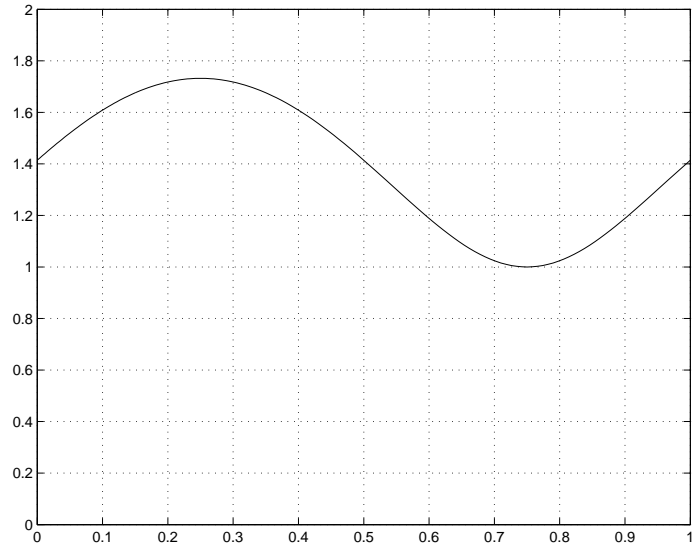


Figure 2: Material coefficient $a(x)$ in the numerical experiment 4.1.

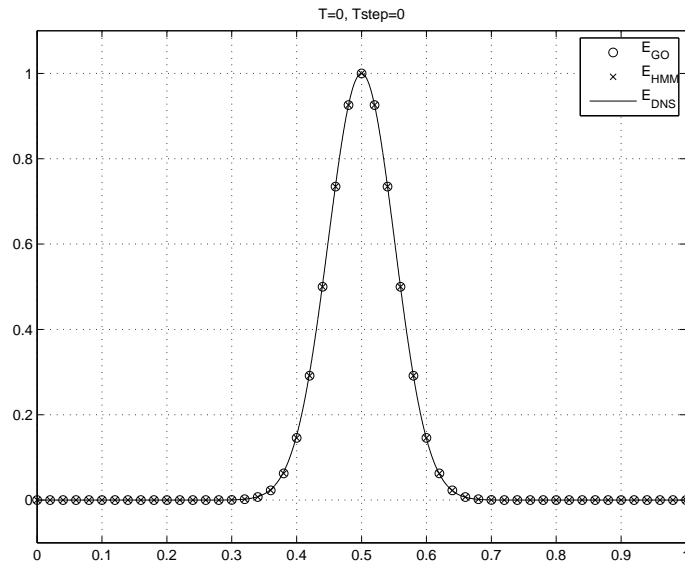


Figure 3: Initial (right-going) energy at $t = 0$ for numerical experiment 4.1.

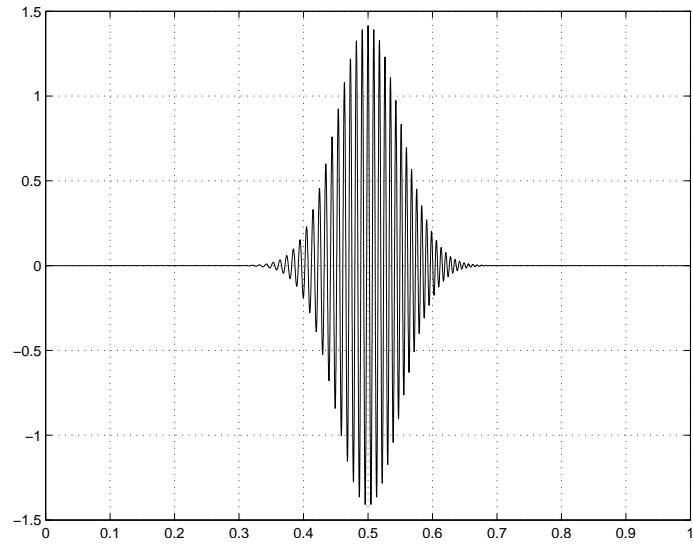


Figure 4: The initial wave u^ε (real part) at $t = 0$ for numerical experiment 4.1.

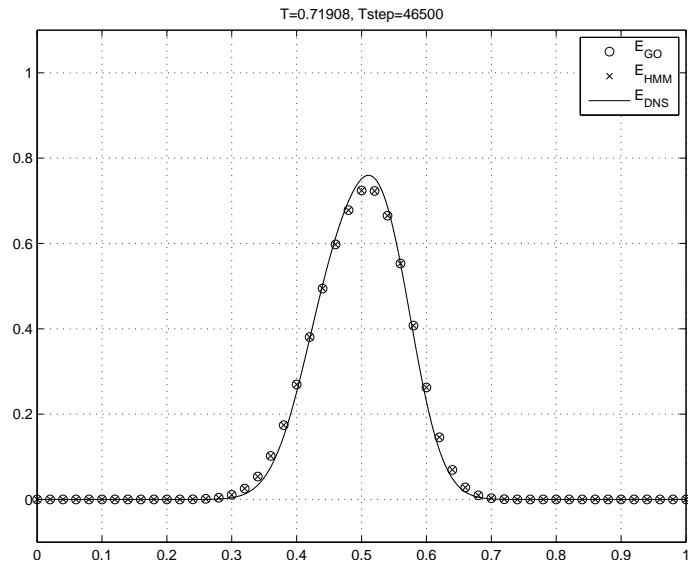


Figure 5: Energy profile at $t = T$ for for the numerical experiment 4.1.

4.2 Numerical experiment two

In this experiment we will consider a wave traveling through a constant medium with $a_0 = 1$ to the left of $x = 0.5$ and $a_1 = \frac{1}{3}$ on the right of $x = 0.5$. The width of the jump is denoted δ . We have constructed $a(x)$ as the square root of $a^2(x)$ where a^2 is continuously differentiable for all $0 \leq x \leq 1$. The form of $a^2(x)$ is,

$$a^2(x) = \begin{cases} a_0^2 & 0 \leq x < -\frac{\delta}{2} + b_0, \\ a_0^2 + (a_1^2 - a_0^2)v\left(\frac{(x-b_0)+\frac{\delta}{2}}{\delta}\right) & -\frac{\delta}{2} + b_0 \leq x \leq \frac{\delta}{2} + b_0, \\ a_1^2 & \frac{\delta}{2} + b_0 < x < -\frac{\delta}{2} + b_1 < x < \frac{\delta}{2} + b_1 \\ a_1^2 + (a_0^2 - a_1^2)v\left(\frac{(x-b_1)+\frac{\delta}{2}}{\delta}\right) & -\frac{\delta}{2} + b_1 \leq x \leq \frac{\delta}{2} + b_1, \\ a_0^2 & \frac{\delta}{2} + b_1 < x \leq 1, \end{cases}$$

where

$$\begin{cases} a_0 = 1, & a_1 = \frac{1}{3}, \\ b_0 = 0.25, & b_1 = 0.75, \\ \delta = 0.0005, & v(x) = -2x^3 + 3x^2. \end{cases} \quad (26)$$

Note that a^2 is made 1-periodic outside $\Omega = [0, 1]$ in some suitable way. We show a graph of a in Fig. 9.

From theory we know that in the limit as $\delta \rightarrow 0$ the amplitude of the reflected wave $u_{\text{ref}}^\varepsilon$ will be of order $\gamma|u_{\text{inc}}^\varepsilon|$ where $u_{\text{inc}}^\varepsilon$ is the incident wave that hits the discontinuity from the left and γ is the reflection coefficient given by [13],

$$\gamma = \frac{a_0 - a_1}{a_0 + a_1}.$$

In the limit of our setup we have $\gamma = 0.5$, i.e. the reflected wave will be half the amplitude of the incident wave.

The interesting part in this experiment is that geometrical optics (GO) fails to capture this reflection effect. The coarse scale GO solution will travel through the jump unaffected.

At the jump $x_m = 0.5$ or $x_m = 0.75$ we use 128 grid points per ε in the micro problem to accurately capture the effects of the jump. For all other macro grid points we use the analytical form that $F^R = aE$ and $F^L = -aE$ to compute the fluxes. For the micro problem we used $\varepsilon = 10^{-3}$, $\eta = \varepsilon$, $\tau = 2\varepsilon$, $\lambda = 0.9$. In this example we did not use a kernel, instead we pointsampled the fluxes at a fixed x outside the jump, on both right and left side, where the outgoing flux is stable and a is smooth (constant in this case). See Fig. 1.

The transmission matrix S in the jump at $x = 0.5$ are,

$$S^R = \begin{bmatrix} -0.75382 & -0.082062 \\ 3.5203e-11 & 0.33333 \end{bmatrix}, \quad S^L = \begin{bmatrix} -1 & 0 \\ 0.24619 & 0.25127 \end{bmatrix},$$

and for the right and left side sampling and for $x = 0.75$ they are,

$$S^R = \begin{bmatrix} -0.25127 & -0.24619 \\ 0 & 1 \end{bmatrix}, \quad S^L = \begin{bmatrix} -0.33333 & 0 \\ 0.082062 & 0.75382 \end{bmatrix}.$$

A visualization of the solution to the micro problem is found in Fig. 1.

We present the initial data and the numerical results at $T = 0.5$ in Fig 6, 7 and 8.

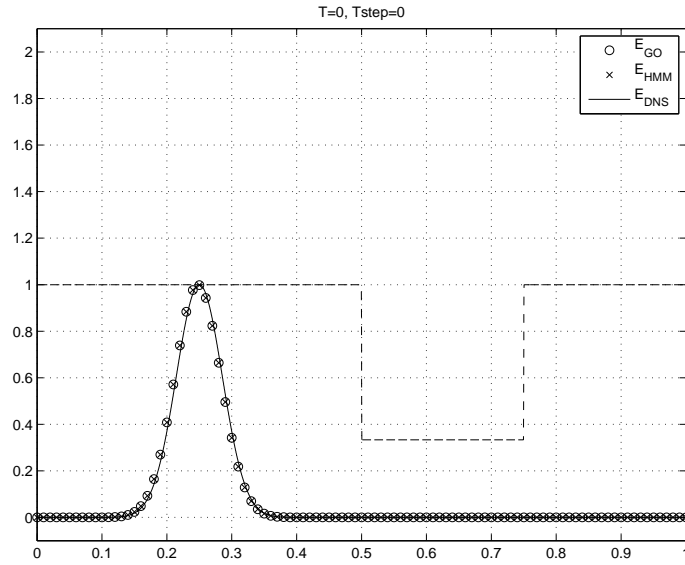


Figure 6: Initial (right-going) energy at $t = 0$ for numerical experiment 4.2.

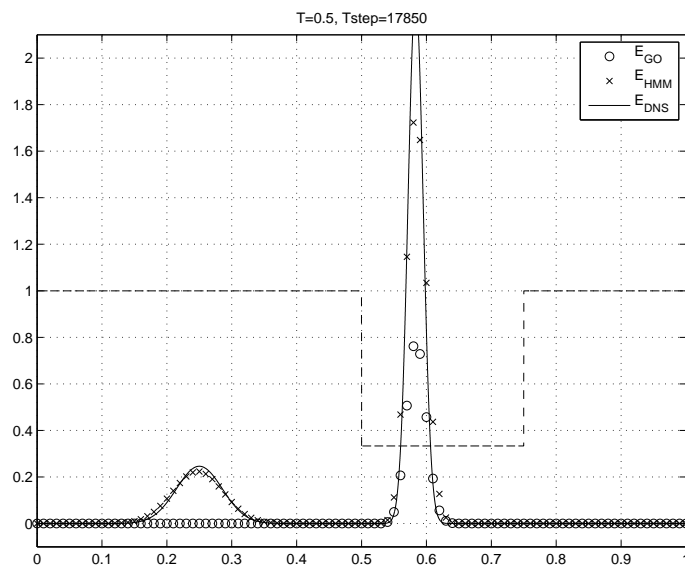


Figure 7: Energy profile E at $t = T$ for numerical experiment 4.2. We see that a smart portion of the energy has been reflected.

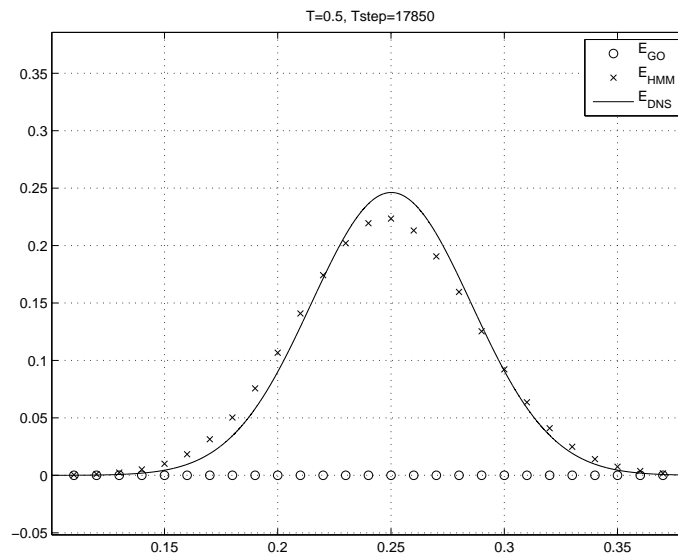


Figure 8: Energy profile at $t = T$ for for the numerical experiment 4.2, zoomed around the reflected energy.

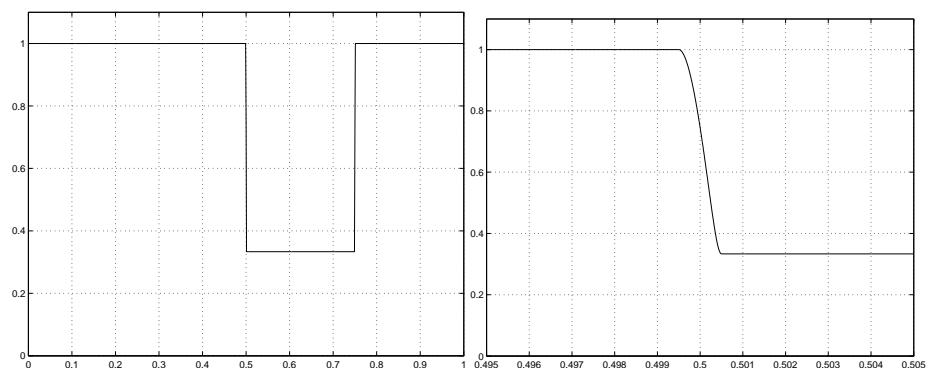


Figure 9: The material used in the numerical experiment 4.2: $a(x)$ plotted over $0 \leq x \leq 1$ with a jump from $a = 1$ to $a = 1/3$ at $x = 0.5$ and another jump from $a = a_1$ to $a = a_0$ at $x = 0.75$.

5 Conclusions

We have developed and analyzed numerical methods for multiscale wave equations with oscillatory initial data. The methods are based on the framework of the heterogeneous multiscale method (HMM) and have substantially lower computational complexity than standard discretization algorithms: The macroscopic PDE is discretized independent of the microscale ε and each micro problem is discretized on a box essentially independent of ε . We presented a numerical example which shows that our method accurately captures the same solution as the geometrical optics (GO) when it is applicable. We also demonstrated that our HMM also captures the correct solution when a has a sharp jump, whereas classical GO fails. We also outlined ideas for extensions to two-dimensions and methods for a non-matched phase function.

References

- [1] Jean-David Benamou. Big ray tracing: Multivalued travel time field computation using viscosity solutions of the eikonal equation. *Journal of Computational Physics*, 128(2):463–474, 1996.
- [2] Jean-Pierre Berenger. A perfectly matched layer for the absorption of electromagnetic waves. *Journal of Computational Physics*, 114(2):185 – 200, 1994.
- [3] Weinan E, Bjorn Engquist, and Zhongy Huang. Heterogeneous multiscale method: A general methodology for multiscale modeling. *Phys. Rev. B: Condens. Matter Mater. Phys.*, 67(9):092101, Mar 2003.
- [4] Weinan E, Bjorn Engquist, Xiantao Li, Weiqing Ren, and Eric VandenEijnden. Heterogeneous multiscale methods: A review. *Commun. Comput. Phys.*, 2(3):367–450, 2007.
- [5] Björn Engquist, Henrik Holst, and Olof Runborg. Analysis of HMM for one dimensional wave propagation problems over long time. 2011, arXiv:1111.2541v1.
- [6] Björn Engquist, Henrik Holst, and Olof Runborg. Multiscale methods for the wave equation. *Comm. Math. Sci.*, 9(1):33–56, Mar 2011.
- [7] Björn Engquist, Henrik Holst, and Olof Runborg. Multiscale methods for wave propagation in heterogeneous media over long time. In Björn Engquist, Olof Runborg, and Richard Tsai, editors, *Numerical Analysis and Multiscale Computations*, volume 82 of *Lect. Notes Comput. Sci. Eng.*, pages 167–186. Springer Verlag, 2011.
- [8] Björn Engquist and Andrew Majda. Absorbing Boundary Conditions for the Numerical Simulation of Waves. *Mathematics of Computation*, 31(139):629–651, 1977.
- [9] Björn Engquist and Olof Runborg. Multiphase computations in geometrical optics. *J. Comp. Appl. Math.*, 74:175–192, 1996.

- [10] Björn Engquist and Olof Runborg. Computational high frequency wave propagation. *Acta Numer.*, 12:181–266, 2003.
- [11] Björn Engquist, Olof Runborg, and Anna-Karin Tornberg. High frequency wave propagation by the segment projection method. *J. Comp. Phys.*, 178:373–390, 2002.
- [12] Björn Engquist and Yen-Hsi Tsai. Heterogeneous multiscale methods for stiff ordinary differential equations. *Math. Comp.*, 74(252):1707–1742, 2005.
- [13] Eugene Hecht. *Optics (4th Ed.)*. Addison Wesley, 2001.
- [14] Henrik Holst. Algorithms and codes for wave propagation problems. Technical report, CSC/NA, 2011.
- [15] Joseph B. Keller. Geometrical theory of diffraction. *J. Opt. Soc. Am.*, 52(2):116–130, Feb 1962.
- [16] J. Qian and L. Ying. Fast multiscale Gaussian wavepacket transforms and multiscale Gaussian beams for the wave equation. *SIAM MMS*, 8:1803–1837, 2010.
- [17] Nick M. Tanushev Tanushev, Richard Tsai, and Björn Engquist. A coupled finite difference - gaussian beam method for high frequency wave propagation. *UCLA CAM Reports (submitted)*, pages 10–40, 2010.